The 6th European sCO_2 Conference for Energy Systems
April 9-11, 2025, Delft, Netherlands

2025-sCO2.eu-193

DESIGN CHALLENGES AND PRELIMINARY TEST RESULTS OF A HIGH TEMPERATURE SUPERCRITICAL CARBON DIOXIDE DRY GAS SEAL TEST RIG

Abdelrahman Abdeldayem
Faculty of Engineering and Applied Sciences, Cranfield University
Bedfordshire, UK

Sajal Kissoon
Faculty of Engineering and Applied Sciences, Cranfield University
Bedfordshire, UK

Eduardo Anselmi Palma
Faculty of Engineering and Applied Sciences, Cranfield University
Bedfordshire, UK

ABSTRACT

Supercritical carbon dioxide (sCO_2) has shown a high potential in power generation cycles to increase thermal efficiency and decrease the physical footprint. Supercritical CO_2 power cycles operate at relatively high temperatures compared to steam and air, necessitating the development of new sealing materials. In this paper, the design challenges, development and preliminary test results of a 500°C, 200 bar sCO_2 dry gas seals test rig are presented. The main rig components are pressure control devices (liquid pump and expansion valves), heat exchangers (liquid condenser, gas heaters, and air cooler), and measuring instruments. Various design challenges are identified due to the thermo-physical properties as well as the operating conditions of the sCO_2 test rig such as the ice formation during start-up, heat loss to the ambient air, and material compatibility with the various test rig components. A thermodynamic design model has been developed to size the test rig components and estimate the gas conditions across the rig. The model includes tube and valve sizing, heat exchanger design, and thermal insulation models. The initial phase of the test campaign was conducted at Cranfield University (CU) to verify the ability of the test rig to deliver sCO_2 at the required conditions and to validate the developed numerical models. The results showed the validity of the proposed setup to supply sCO_2 steadily at 500°C and 200 bar at a flow rate of 15 kg/h. The heat exchanger model applied to a finned tube bundle air cooler showed close estimations to the test results with a maximum deviation in the heat capacity of 2.3%. The thermal insulation model including the heating tape showed reasonable predictions for the temperature rise across the heating sections with a maximum deviation from the experimental measurements of 10°C when the temperature rise was around 240°C. The suitability of using rock wool insulation and stainless steel 316 tubes with dry CO_2 at 500°C was verified.

KEYWORDS

Supercritical CO_2, experiment, dry gas seal, modelling.

1 INTRODUCTION

Supercritical carbon dioxide (sCO_2) power cycles are redefining energy conversion technologies due to their exceptional thermodynamic properties and their ability to operate efficiently for a wide range of applications [1], [2]. In thermodynamic cycles, sCO_2 has gained popularity due to its high density and low compressibility near the critical point, resulting in reduced compression work and less hydraulic losses [3]. Additionally, CO_2 is readily available, non-toxic, thermally stable at elevated temperatures and has a wider operating temperature range [4]. Supercritical CO_2 power cycles can theoretically achieve higher thermal efficiencies compared to traditional working fluids such as steam and air however, sealing sCO_2 turbomachinery is challenging due to the high operating temperatures of these cycles [5]. Furthermore, the high density and low viscosity of sCO_2 increase the impact of both external and internal leakage on the thermal efficiencies of the specific cycle components [6].

The elevated temperature of sCO_2 power cycles limits the spread of sCO_2 in turbomachines with conventional labyrinth seals [7], [8]. In addition, these temperatures complicate the cooling system design of the dry gas seals in turbomachines to satisfy the market limits near 220°C [6]. Various research activities targeting the development of high temperature dry gas seal components are presented in the literature. Nielson et al. [9] tested different types of balance sealing components that allow the axial movement of the stationary ring. The test rig is composed of a CO_2 source, a pressure regulator, a pressure chamber that accommodates the sealing element and a radiant heater. Over 10 balance seal assemblies are tested at ambient temperature while only one type is selected for a high temperature test at 500°C and 74 bar. While the proposed rig design can achieve high temperatures, the supplied gas pressure is limited to the bottle pressure when the pressure regulator valve is fully open.

Furthermore, sCO_2 seal test rigs are presented in the literature with the testing temperature limited to 250°C [10],

* a.s.abdeldayem@cranfield.ac.uk

DOI: 10.17185/duepublico/83294

[11]. Steinmann et al. [10] and Rimpel et al. [11] presented their test rigs which are designed to test static and dynamic seal rotation with the maximum pressure of 285 bar and 75 bar, respectively. Other test rigs were presented in the literature with a testing temperature limited to 160ºC, 110ºC, and 76.6ºC as illustrated by Laxander et al. [12], Yan et al. [13], and Cich et al. [14], respectively.

Research into the development of an innovative, uncooled high-temperature dry gas seal (DGS) solution specifically tailored for supercritical CO_2 power cycles was undertaken collaboratively by John Crane, Cranfield University and the University of Edinburgh as part of the Carbon Capture, Usage and Storage (CCUS) Innovation 2.0 program CCUS 2108 [15]. The project scope includes the design, fabrication, and laboratory testing of critical DGS components (balance diameter sealing module) and system prototypes for application in rotating equipment (turbine and compressors) used in sCO_2 power cycles up to typical pressures and temperatures of 200 barg and 500ºC. The project also includes the design and commissioning of test equipment to verify and demonstrate the innovative DGS concept/ prototype.

This paper details the design and manufacturing process of a high temperature sCO_2 test rig, designed to supply a steady sCO_2 mass flow of 15 kg/h, 500 ºC at 200 bar for testing dry gas seal components. The major design challenges associated with the working fluid and operating conditions are thoroughly discussed. Furthermore, the numerical model results, experimental setup and preliminary test results are presented. The aim of this experimental activity is to evaluate the rated performance of the various test rig components, assess the insulation and heating capabilities, evaluate the cooling performance of the proposed cooling bundle, and test the accuracy of the back pressure control devices. Furthermore, the system's response to control actions is assessed to quantify the required startup time and possible overshooting of the test conditions.

2 DESIGN CHALLENGES & PROPOSED STRATEGIES

Various design challenges are identified due to the high pressure and temperature requirements of the test rig. The high design temperature of 500ºC limits the material selection process of the various test rig components. Stainless steel 316 (SS 316) is commonly used for tubes, fittings and valve bodies, due to its wide availability and short lead time in the market. However, most tube manufacturers recommend using SS 316/316L below 537ºC as the pressure rating of components drops sharply after this limit, resulting in a potential mechanical failure [16]. To address the temperature limitations of SS 316, alternative materials capable of withstanding higher temperatures were considered. Inconel 625 was found promising however, it has a long lead time in the UK market and has a limited variety of fittings compared to SS 316. Furthermore, Inconel 625 requires more sophisticated bending and welding processes which negatively impacts the overall project cost and time frame. These considerations led to the decision to use SS 316, with the sCO_2 temperature strictly limited to 500ºC at all points across the rig. This limitation introduced additional constraints to the heating control process to prevent overshooting beyond the allowable threshold. Additionally, compensating for heat loss by supplying the gas at temperatures exceeding 500ºC is no longer feasible while the gas must be maintained at a constant temperature across the hot tube section presented in Figure 1 by section A. Section B represents another challenge where the hot gas coming out of the cell should be sufficiently cooled before approaching the downstream components.

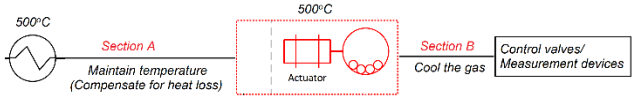

Figure 1 Cooling and heating challenges

Maintaining high temperatures over extended tube sections is challenging due to the significant heat losses to the surrounding air. Additionally, the thermal conductivity of insulation materials deteriorates at elevated temperatures. For instance, the thermal conductivity of Rockwool fibre insulation increases from 0.04 W/m·K at room temperature to 0.11 W/m·K at 500°C. Identifying thermal insulation suitable for 500°C is particularly challenging due to the limited market availability, as the commonly available insulation materials are designed and tested for lower temperatures, such as HVAC applications. The challenge becomes even greater for small-diameter tubes. One viable option is found the mineral Rockwool fibre insulation, which is available for pipe diameters from as small as 15 mm. For tubes of a ¼" (6.35 mm) outer diameter, a gap of approximately 4.3 mm is formed between the tube and the insulation. To address this, a suitable packing material must be identified to effectively fill the gap and enhance the thermal insulation.

To address the challenge of maintaining the temperature of the hot tube section constant near the upper limit of 500ºC, an innovative solution is proposed using a heating tape that is available in the market in various sizes to either heat the gas or compensate for the temperature losses. These electric resistance heating elements can withstand high temperatures up to 700ºC and can fill the gaps between the tubes and the insulations material, leading to a perfect heating section. This heating section composed of the heating tape and the pipe insulations makes a perfect combination that satisfies the testing requirements with low cost, short lead time, easy manufacturing, and flexible adjustable solution.

The high operating temperature introduces complications to selecting the packing material of the control valves as most of the commercial SS 316 valves using traditional packing materials, such as Polytetrafluoroethylene (PTFE), are

DOI: 10.17185/duepublico/83294

limited to ~300ºC. A few tube manufacturers offer Grafoil packing to increase the valve temperature limit to ~450ºC however, expanding the gas from 500ºC is unrealistic. As a solution to this challenge, coolers are designed to cool the gas before approaching the valves and measurement devices to meet the temperature limits specified by the manufacturers. The cooling bundle is made from the same tubes used to connect the system components. The fines, made of SS 316, are shrink-fit to the tubes, minimising the thermal contact resistance between the fins and the tube walls without the need for any bonding agents.

Operating at high pressure introduces challenges such as ice formation and the potential line blockage when expanding the gas below the triple point temperature of CO_2 near -56ºC. In addition, the high-pressure ratio leads to a choked flow which limits the mass flow control options for controlling the valve flow coefficient (Cv) as changing the valve outlet pressure has no effect on the mass flow rate within the choked range.

Effective mass flow control is critical to maintaining operational compatibility between the expansion device and the pump, which is designed to sustain a constant pressure equal to the test pressure. Given the limited availability of a flow control valve capable of operating at the required design pressure, temperature and mass flow rate, initial testing relies on manual control of the metering valve. This setup is later enhanced with an automated system, integrating a stepper motor with the metering valve and connecting it to a PID controller for precise regulation.

The data acquisition and control process is also challenging due to the strict design and operation requirements. The heating control must have a minimal temperature overshooting, especially when operating at 500ºC because that is close to the manufacturer's defined limit of 537ºC for SS 316. At the same time, the response to the temperature change should be reasonably fast to avoid wasting CO_2 to the ambient for this specific application where the working fluid is not recycled. The control speed is also important to ensure supplying the gas at the required conditions to allow testing a wide range in a realistic time frame. The measurements and instrumentation are also challenged by the high operating temperature where special care should be given for the selection and installation of the sensors and actuators. To mitigate the impact of high temperature on the sensors, static devices, such as the pressure sensors, are located away from the main lines using coils made of the same rig tubes. Other devices are relocated whenever possible to ensure safe operating temperatures.

3 EXPERIMENTAL SETUP

The test setup presented in this paper is a simplified version of the actual test aiming at testing dry gas seal materials at high pressure and temperature combinations. In the current test, the sCO_2 gas supply is designed to evaluate the test rig components at a total flow rate of ~15 kg/hr. Two streams of gas were designed to simulate the leakage and continuous flow lines of the actual test, while only one line is used in this test campaign as this can reasonably verify the validity of the proposed back pressure control system. The P&ID of the test campaign is shown in Figure 2.

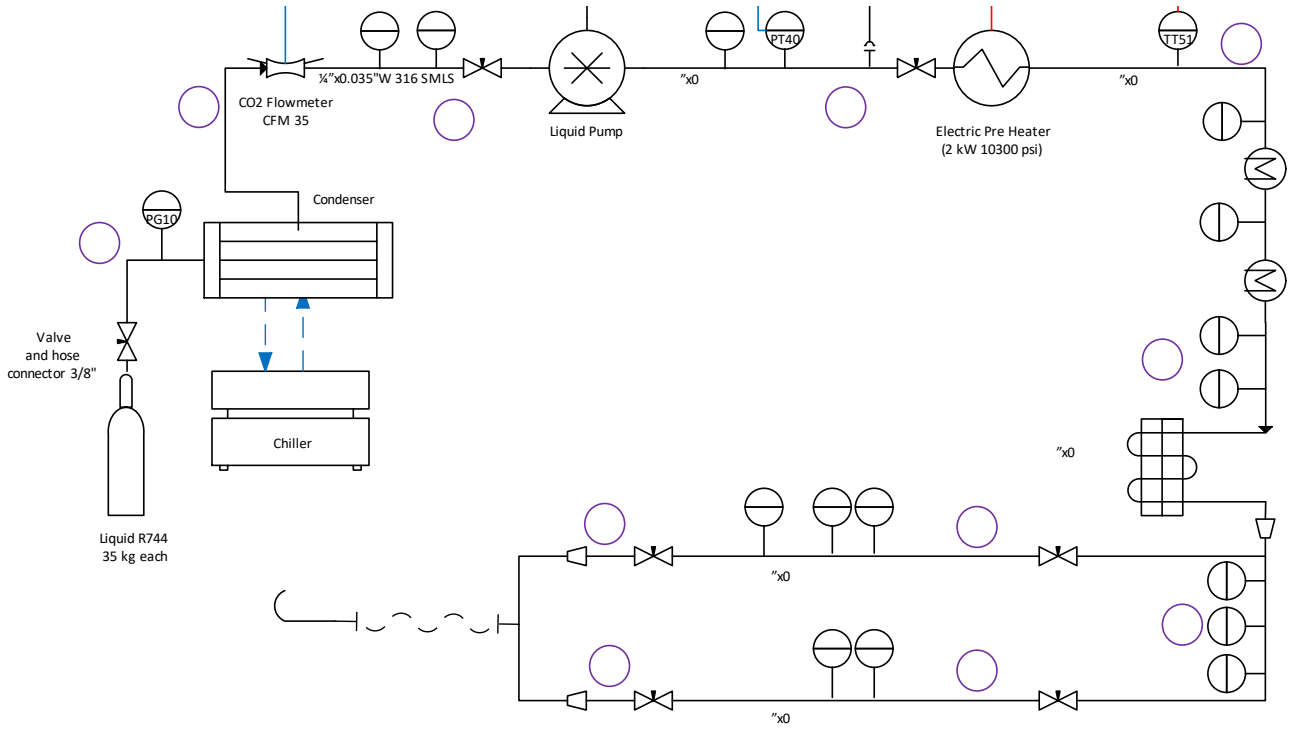

DOI: 10.17185/duepublico/83294

The components utilised in the test include a bottle of liquid R744, ~35 kg, a water chiller and a liquid CO_2 pump equipped with a condenser to make sure that the pump suction is subcooled liquid. Two electric heating stages are utilised with a 2kW Electric preheater, and two sections of tubes covered with electric resistance heating tape, 940 W each. The gas is then cooled in a finned cooling bundle and expanded in a metering valve SS-31RS4-G. A needle valve SS-3HNRS4-G is then used for shutting off purposes. The main system components and their relative positions in the test area are shown in Figure 3 and Figure 4. The back pressure control devices as well as the measuring devices are integrated in a panel located next to the pump unit. In addition, the panel is equipped with a variable AC switch to control the power supplied to the heating tape.

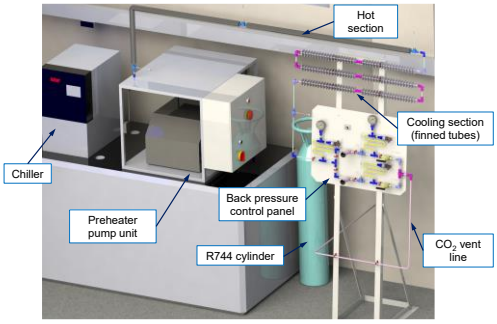

Figure 3: The 3D design of the test campaign rig.

Figure 4: Picture of the test rig showing the heating section, the cooling bundle and the control/measurement devices.

4 NUMERICAL MODELS

4.1 HEAT LOSS AND THERMAL INSULATION

To assess the heat lost from the insulated tubes, a steady-state heat transfer model is developed, considering the heat dissipation by natural convection to the ambient air. The test tube has a 0.25" outer diameter (Ø1/4") with a wall thickness of 1.651 mm. The ambient temperature is assumed at 20ºC while the flow inside the tube is CO_2 with a variable inlet pressure and temperature. The pressure varies between ambient and 200 bar while the temperature varies between ambient and 500ºC. The mass flow rate varies between 2kg/hr and 20kg/hr to cover the expected testing range. The insulation material is foil-faced rock mineral wool with a thermal conductivity of 0.15 W/m.K at a temperature range from 200ºC to 500ºC [17]. The insulation layer thickness is 30 mm with an internal diameter of 15 mm.

The model solves the energy equation to evaluate the temperature distribution across the tube section using the concept of thermal resistances. The heat transfer coefficients are calculated based on the external flow correlations for the ambient air and the internal flow correlations for the CO_2 as presented by Cengel and Ghajar in chapters 8 and 9 for the forced and natural convection, respectively, [18]. The results of the model are summarised in Figure 5 for different inlet temperatures and pressures. In this figure, two pressure values are selected corresponding to heating near the ambient pressure and heating at the pressure of 200 bar. Two inlet temperature values are selected corresponding to heating from ambient temperature at 20ºC or from the preheater outlet temperature of 200ºC. The heating section outlet temperature is limited to 500ºC, represented by the solid red line, by limiting the heating power supply. The dashed red line shows the maximum achievable outlet temperature at full power. The blue lines represent the actual heat transfer values corresponding to the limited temperature (T_2).

Increasing the mass flow rate decreases the maximum achievable temperature at the heating section outlet ($T_{2,max}$) and increases the useful heat gain for the four cases. At a flow rate near 15 kg/hr, the useful heat gain increases from 79% to 86% when the operating pressure increases from 1 bar to 200 bar however, the maximum outlet temperature (T_2) drops from 396ºC to 230ºC due to the increased fluid density. Increasing the inlet temperature increases the outlet temperature from 230ºC to 450ºC when operating at 200 bar and 15kg/hr, which significantly improves the heating capabilities although the heat loss increases, and the useful heat gain decreases due to the high inlet temperature.

In summary, the highest outlet temperature is achieved at the low pressure, high inlet temperature case while the best heating efficiency, represented by the maximum useful heat gain, is achieved by the high pressure, low inlet temperature case.

DOI: 10.17185/duepublico/83294

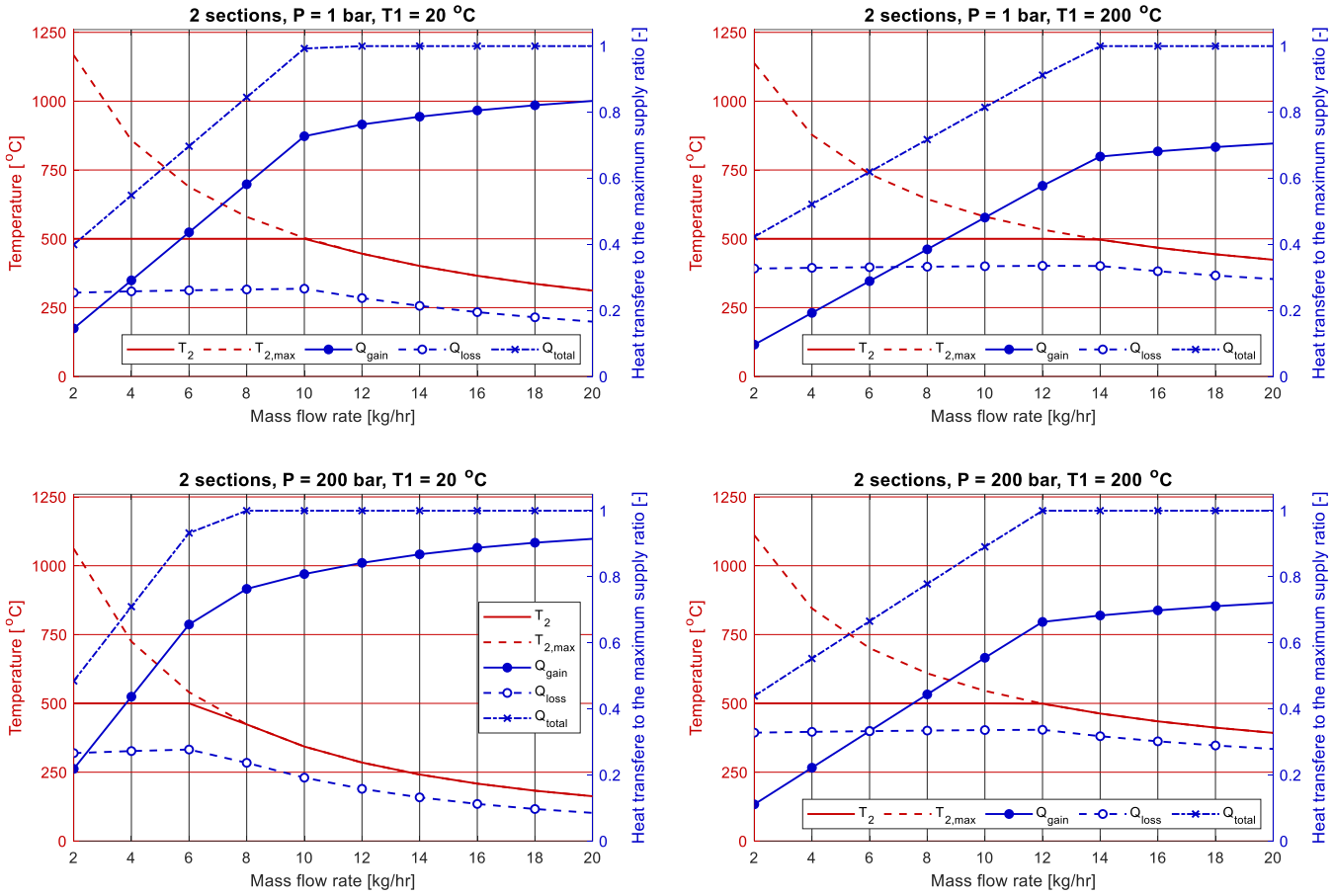

4.2 FINNED BUNDLE MODEL

A cooling bundle has been designed and manufactured to lower the CO_2 to a safe operating temperature, protecting the rig components installed downstream of the heating section. This solution offers a simple yet efficient alternative to purchasing a heat exchanger from the market, where high operating pressures and temperatures would result in high costs and extended lead times. The 3D model of the fined tube bundle is shown in Figure 6 and the geometrical details are given in Table 1. The same tubes used to connect the CO_2 pump with the test rig are used to manufacture the tube bundle in-house. The bundle consists of 6 units, with each unit having 20 fins. The entire assembly offers a total surface area of 0.47 m^2 compared to 0.08 m^2 of the bare tubes.

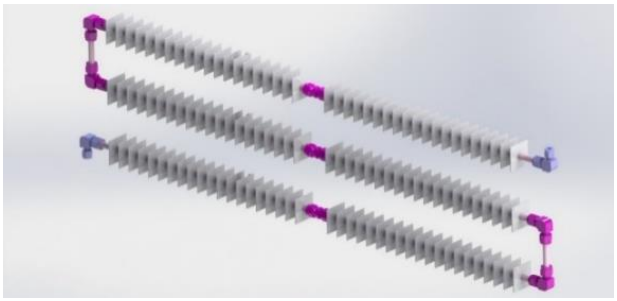

Figure 6: Finned tube bundle geometry with fittings.

Table 1: Finned tube bundle geometry.

Parameter	Value
Tube outer diameter	3/8"
Tube wall thickness	0.065"
Number of tube units	6
Tube unit length	45 cm
Number of find per tube unit	20
Fin thickness	1.6 mm
Fin spacing	20 mm (face to face 18.4 mm)
Fin geometry	Square of side length 40 mm
Fin hole size	9.5 mm (shrink fit 25 microns)

A numerical model has been developed using MATLAB to estimate the cooling performance of the finned tube bundle. The model calculates the fins efficiency of the rectangular fins similar to the commonly used annular fins [18]. The normal operating conditions are tested where the inlet temperature, inlet pressure, and mass flow rate are 500°C, 200 bar, and 15 kg/hr. In this case, the inlet velocity is 1.0279 m/s

DOI: 10.17185/duepublico/83294

and the outlet velocity is 0.5133 m/s. The calculated temperature drop across the tube bundle is 307.7°C, resulting in an outlet temperature of 192.3°C and a total heat loss from the finned bundle of 1610 W.

A parametric study has been carried out to understand the bundle performance at different operating conditions as shown in Figure 7. In this study, the mass flow rate ranged from 2 kg/h to 20 kg/h, with operating pressures set at 200 bar, 100 bar, or atmospheric, and inlet temperatures of either 300°C or 500°C. A significant amount of heat loss is observed, which increases with a decrease in mass flow rate or an increase in inlet temperature. Reducing the operating pressure decreases the gas density and increases the velocity, resulting in a higher rate of heat transfer, and increases the temperature drop across the cooling bundle. Increasing the inlet temperature results in a higher temperature difference between the flowing gas and the ambient. Consequently, the temperature drops and the total heat transfer increases.

By evaluating the expected leakage flow during the seal test of ~5 kg/hr, this stream can be cooled down to 55°C from an inlet temperature to the bundle of 500°C at ambient pressure. At higher leakage rates, i.e. 10kg/hr, the cooled stream temperature is 120°C. Further cooling can be achieved by using a fan to circulate the high and achieve higher heat transfer coefficients.

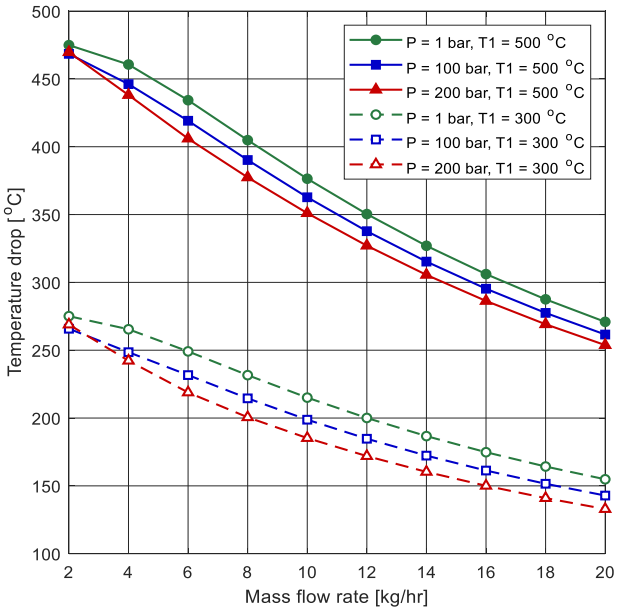

Figure 7 Cooling bundle performance at variable pressure and inlet temperature

4.3 BACK PRESSURE SIMULATION MODEL

Following a broad survey of the features and costs of back pressure regulators available on the UK market, it was decided that as a proof of concept, the first approach would involve a simple combination of metering valves and needle valves to control flow and pressure downstream of the test apparatus. The principle behind this approach relies on the fact that commercial back pressure devices offer very low valve sizing coefficients (Cv), in the range of 1E-6 to 0.10, which can be reproduced by metering valves. A downstream needle valve enables the control of pressure downstream of the metering valve when it needs to be other than ambient. Using features of Simscape® Simulink [19], a numerical model was developed to estimate the mass flow, pressure, temperature, and Mach number across this arrangement. Another important feature of the model was the prediction of the number of turns to open/close the metering valve. Two metering valves were assessed in detail: 30VRMM4812 made by Parker [20] and SS-31RS4-G (Grafoil Packing) made by Swagelok [21]. Previously published results by Yuan and Anderson [22], which specifically addressed carbon dioxide as the working fluid, encouraged the selection of the second option for testing. The SS-31RS4-G valve Cv is shown in Figure 8.

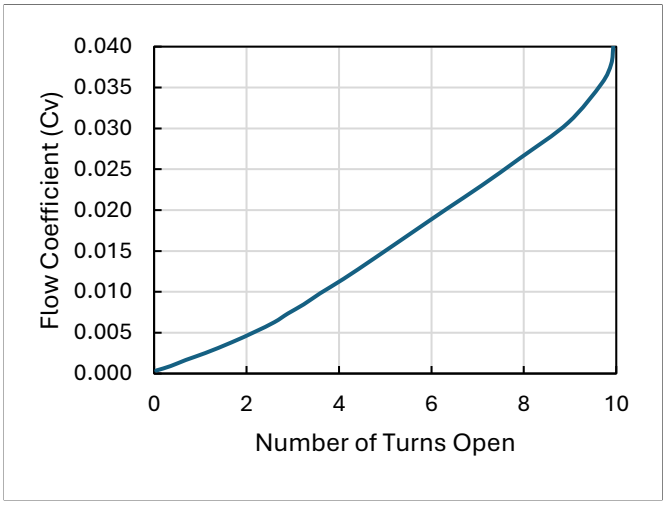

Figure 8 Cv curve - Swagelok SS-31Rs4-G valve [21].

To verify and calibrate the Simscape model, comparisons were made against results published by Yuan and Anderson [22]. Specifically, those experimentally performed at 50% valve open and a pressure expansion ratio of 0.4. A back-to-back comparison can be seen in Figure 9.

The limitation in establishing more verification points in the simulation model is primarily due to inconsistencies in the physical modelling. Even the source of comparison (Yuan et al. [11]) recognised that the complexity of real-world phenomena could not be captured with their theoretical or modified gas valve models (values of Cv equal to 0.015 or 0.02 in each case). Underestimation and overestimation of mass flow versus experiments were common, pointing out limitations due to the choked-flow method followed. Although the Simscape model reproduced similar trends, it consistently underestimated the pressure differential ratio required at choked conditions $(P_1-P_2)/P_1$ (represented by the xT* coefficient) to match the Cv value.

DOI: 10.17185/duepublico/83294

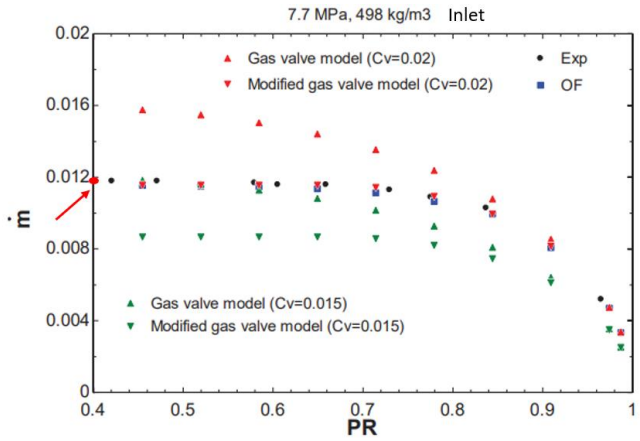

Figure 9 Comparison between the metering valve Simscape model results with Yuan et al. [23]. Cv = 0.015, PR = 0.4.

These inconsistencies arise from several factors: simplifying assumptions in the Simscape environment, the interdependency of variables, and the inherent complexity of the physical processes involved in the operation of the choked system, which may not be fully captured by the current modelling techniques. Despite these challenges, the current verification points provide a reasonable level of confidence in the simulation model's accuracy. Ongoing efforts to refine the model, obtain higher-quality experimental data, and enhance measurement techniques will help address these inconsistencies and improve the model's reliability.

4.4 TEST RIG

The overall performance of the test rig components is modelled and connections between the various components are built to evaluate the overall system performance. These calculations are important because they help predict the gas behaviour at each location of the test rig, including possibilities of ice formation and physical blockage of components. The thermal model is developed to match the process described in Figure 2. However, only a single venting line is utilised, as it is deemed sufficient for evaluating the performance of the back pressure control valves, given that both lines are identical. The results of pressure, temperature, line diameter, and gas velocity are summarised in Table 2. It can be noted from the table that the minimum temperature is obtained at the condenser outlet which has the same pressure as the R744 cylinder, around 50.8 bar. The temperature at the ambient pressure downstream of the needle valves is still sufficiently high to avoid any ice formation, which happens when the gas temperature drops below the triple point temperature of the pure CO_2 (-56°C). Although the expanded gas temperature in this steady state model is sufficiently high, the system transient startup may result in ice formation downstream of the metering or the needle valves due to the low startup temperatures. The gas velocities are calculated based on the line diameters given in the table and a mass flow rate of 15 kg/hr. It can be seen from the table that the maximum velocity is obtained at the outlet of the metering valve where the gas is expanded near the ambient pressure. The velocity at this point is 144.7 m/s which suggests that problems such as noise should be carefully considered during the test. Other high gas velocity problems such as pressure drop and heat loss may not be critical in this case because the tube sections between the components are relatively short.

Table 2: Numerical model results of the test rig.

Description	Pressure [bar]	Temp. [°C]	OD [in]	Velocity [m/s]
[1] Feed line	54.7	18.0	0.500	0.1
[2] Condenser outlet	54.6	6.0	0.250	0.6
[3] Pump suction	54.5	6.0	0.250	0.6
[4] Pump discharge	200.2	18.4	0.250	0.6
[5] Pre-heater outlet	200.1	271.2	0.250	2.8
[6] Hot Section outlet	200.0	500.0	0.250	4.3
[7] Bundle outlet	200.0	194.1	0.375	0.5
[8] Metering out	2.9	119.7	0.250	144.7
[9] Vent	1.0	118.7	0.375	99.9

The test results are further illustrated using the temperature-entropy (T-s) diagram shown in Figure 10. The heating process is represented by the preheater process from 4 to 5 and the heating tape wrapped around the hot section tube from 5 to 6. This process is considered isobaric with a minimal pressure drop of nearly 0.1 bar across both the preheater and the hot section. The cooling process is conducted using the finned tube bundle between stations number 6 and 7 at constant pressure as the tubes of this bundle are fabricated of larger diameter tubes which would significantly decrease the pressure drop of the preheater and hot section. The tubes of the cooling bundle are made of Ø3/8" tubes with 1.651 mm wall thickness compared to Ø1/4" tubes used for the preheater and the hot section of the same wall thickness.

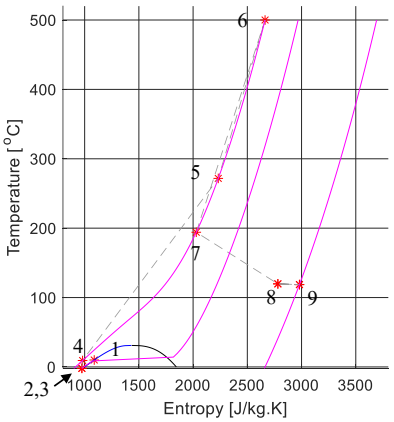

Figure 10: Numerical model results of the test campaign represented by the temperature-entropy diagram.

The metering valve firstly expands the gas at a constant enthalpy from the test pressure of 200 bar to nearly 2.9 bar

DOI: 10.17185/duepublico/83294

which represents the pressure drop across the needle valve due to its low Cv value of 0.05 when fully open. When the mass flow rate is 15 kg/hr, the inlet temperature is 119.7°C, and the outlet pressure is 1 bar, the fully open needle valve results in a pressure drop of 1.9 bar.

5 EXPERIMENTAL RESULTS

5.1 TEST PROCEDURE

The startup process faces challenges due to ice formation when CO_2 expands from ambient temperature and high pressure (~55 bar) to ambient pressure. To address this, electric heaters are preheated to approximately 150°C before gas flow begins. During startup, freezing may occur on downstream tubes, requiring defrosting before resuming operation. The metering valves regulate gas flow, allowing hot gas to warm the system components, and ensuring ice-free expansion. The pump startup involves liquid subcooling using a water chiller to prevent gas from entering the pump.

To achieve the target test conditions, the pump pressure is set to 200 bar, and heating elements (preheater and heating tape) are adjusted to maintain system temperatures. Once steady-state operation is reached, the system is allowed to supply sCO_2 at 15 kg/hr, 200 bar, and 500°C for at least one hour.

5.2 TEST RIG PERFORMANCE

The experimental results are obtained to verify the numerical models and validate the test objectives. The test rig is controlled using a set of control signals to the pump in the form of pressure set point, the preheater in the form of target temperature, the heating tape in the form of applied voltage, in addition to manual control of the metering and needle valve opening. The system performance is monitored using a set of sensors. Thermocouples type K are used which provide a wide range from 0°C to 1100°C with an accuracy of ± 1.5℃. Pressure sensors vary in range between 250 bar for the high-pressure tube sections and 16 bar for the low-pressure and venting lines. The accuracy of the pressure sensors is $\leq \pm 0.2\%$ of the span for the electrical signal plus $\leq \pm 1\%$ for the reading. A Coriolis flow meter is used to measure the mass flow rate of the liquid CO_2 supplied to the pump with an accuracy estimate of $\leq \pm 0.1\%$. Both physical and electrical emergency stops are installed for the pump and preheater unit in addition to a 16A circuit breaker to ensure a safe operation.

The results are reported against time as shown in Figure 11 and Figure 12. In this test run, only the leakage line is operative while both the metering and needle valves installed on the continuous flow line are fully closed. In Figure 11, the input signals of the pump pressure (PP_{sp}), preheater temperature set point (PH_{sp}), heating tape voltage (HT_V), and the metering valve opening turns (MV) are shown against the readings from the various sensors. The pressure and temperature sensors shown in this figure are for the condenser pressure (P_c), pump discharge pressure (P_p), preheater outlet temperature (T_{ph}), intermediate temperature between the two heating tape elements (T_{int}), maximum temperature at the end of the hot section (T_{max}), and the cooled temperature after the cooling bundle (T_{cooled}). Furthermore, the flow meter measurements of density (ρ_{FM}) and mass flow rate (m_{FM}) are plotted and compared to the mass flow rate calculated from the pump rotational speed (m_P).

The target of this test run was to define the mass flow rate at which the maximum temperature is 500°C and maximum pressure is 200 bar when operating the heating devices at full power. It can be noted from the input signals that the steady state operation was achieved after ~12:30 PM. At this point, the input to the pump, preheater, and heating tape is at 100% which represents 200 bar for the pump, 2000W for the preheater power, and 236V across the heating tape terminals. To reach the steady state operation, the metering valve is manually controlled to maintain the maximum temperature at 500°C. It can be seen from Figure 11 that the signal logged for the metering valve opening can be approximated by a converging PID control signal with around 0.3 turns undershooting, 45 minutes damping time and a steady oscillation of less than 5°. It is also worth mentioning that the Simscape model predicted that the operation of the metering valve would range from ½ turn to 2 turns in order to satisfy mass flow values between 4.22 to 16.90 kg/hr when Cv is equal to 0.005.

The pressure sensor installed downstream of the pump discharge (PP_{SP}) indicates the pump response and accuracy which is found satisfactory in building up the pressure during the transient start up and achieving the pressure set point at the steady state operation. The condenser pressure sensor shows a drop in the cylinder pressure as the test progresses due to the gas depletion from the cylinder. This drop in pressure is linked to a drop in the temperature of the gas cylinder over time. The pressure drop of the condenser is measured at 5 bar per hour at the steady-state gas supply of 15 kg/h. Although the pump can compensate for the drop in the cylinder pressure, this can only be achieved as long as the CO_2 is supplied to the pump as a pure liquid. After a certain period of operation, a small percentage of gas starts getting into the pump which fails to satisfy the pressure set point and the flow rate starts to drop. This issue can be overcome by installing multiple gas cylinders in parallel to ensure a continuous supply over longer periods of time.

The temperature measurements reported in this figure show that the target set point of 500°C can be satisfied and maintained steadily for a long period of time exceeding 1 hr which should be sufficient for the seal test in the future testing phases. It has been noted that the temperature response of the preheater (T_{PH}) is slow compared to the response of the two sensors installed downstream of each heating tape to measure T_{int} and T_{max}. Between 12:00 and 12:30, varying the input voltage (HT_V) significantly influences the two temperature

DOI: 10.17185/duepublico/83294

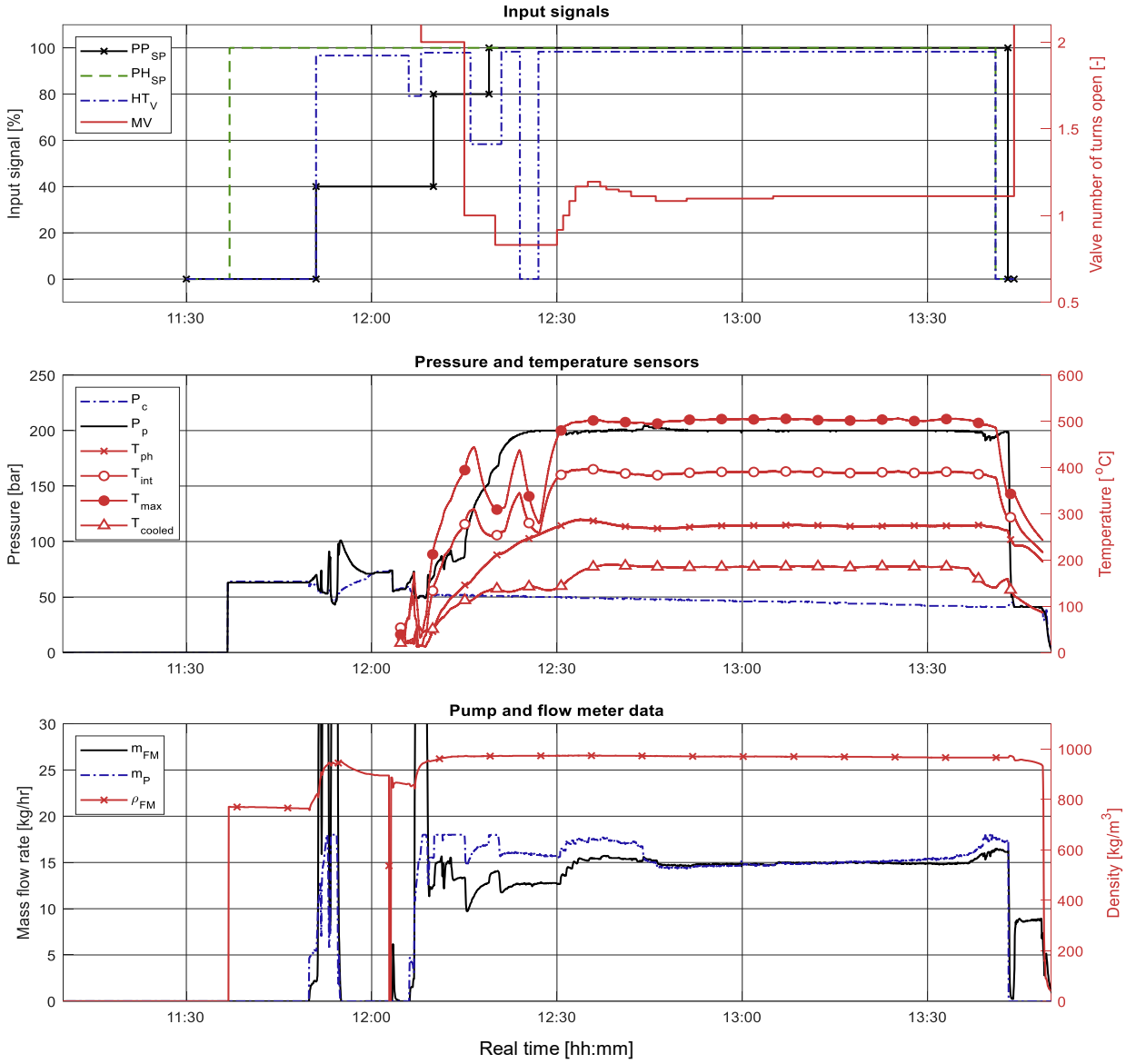

curves, T_{int} and T_{max} , which respond rapidly to changes. The observed cooling performance highlights the effectiveness of the cooling bundle in reducing gas temperature. This capability alleviates restrictions related to the selection of measurement devices and control valves. At steady state, the cooling bundle achieves a temperature drop of approximately 317°C, compared to the 306°C predicted by the numerical model of the finned bundle.

The comparison between the measured and calculated mass flow rate shows a close estimation during the steady operation near 15 kg/h. However, deviations are observed at startup and transient operating conditions due to the differences in density and gas pressure buildup in the different rig components. The liquid density measured during this test is nearly constant between 12:30 and the end of the test indicating that liquid is continuously supplied to the pump and the cylinder still has enough amount of CO_2 for the test.

5.3 FLOW CONTROL PERFORMANCE

The performance of the flow control metering valve is assessed based on the pressure and temperature measurements taken upstream and downstream of the valve, as shown in Figure 12. The metering valve inlet pressure, outlet pressure, inlet temperature and outlet temperature are defined as PM_{in}, PM_{out}, TM_{in} and TM_{out}, respectively. The ambient pressure (P_{amb}) is highlighted by a dashed green line to indicate the pressure drop across the needle valve installed downstream of the metering valve. It can be seen from the figure that the metering valve can maintain a steady pressure drop between 200 bar at the inlet and nearly ambient outlet. Under these pressure conditions, the temperature drop across the metering valve is around 100°C from 185°C at the cooling bundle outlet to 80°C downstream of the metering valve. During the steady-state gas supply, the pressure drop across the needle valve when fully open is 1.9 bar.

DOI: 10.17185/duepublico/83294

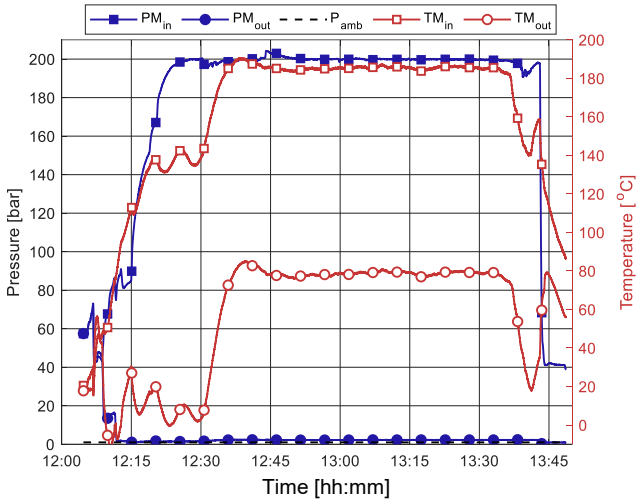

Figure 12 The change of the metering valve parameters over time.

5.4 COMPARISON BETWEEN NUMERICAL AND EXPERIMENTAL RESULTS

A comparison has been made between the numerical models' predictions and the experimental results. The results in this comparison are obtained when the system is steadily running at 200 bar, 500°C, and 15 kg/h. The performance metrics of the different system components are listed and compared in Table 3. The sensor tags used in this table refer to the numbering in the PID diagram shown in Figure 2.

A good agreement is observed between the results for the preheater, heating tape, and cooling bundle predictions. However, the temperature drop across the metering valve is underestimated by the numerical model due to the adiabatic expansion assumption, neglecting the heat loss from the valve body and the inlet/outlet tube connections and fittings. Overall, the results show a satisfactory modelling accuracy that aligns with the obtained experimental measurements.

Table 3: Performance metrics of the test rig components.

Component	Performance metrics	Exp	Num	Err%
Preheater	Outlet temp ($TT51$) [°C]	275.1	271.2	-0.7%
Heating tape	Intermediate temperature ($TT53$) [°C]	390.5	392.0	0.2%
Heating tape	Outlet temp ($TT61$) [°C]	502.0	500.0	-0.3%
Insulation	Surface temperature [°C]	85.0	98.3	3.7%
Cooling bundle	ΔT ($TT61 - TT71$) [°C]	316.6	305.9	-1.8%
Metering valve	ΔP ($PT70 - PT80$) [bar]	197.1	197.1	0.0%
Metering valve	ΔT ($TT71 - TT81$) [°C]	107.0	74.4	-8.6%
Fully open needle valve	ΔP ($PT80 - Patm$) [bar]	2.0	1.91	-4.5%

6 CONCLUSION

The test results of a sCO_2 dry gas seal test rig designed to supply CO_2 at 200 bar and 500°C are presented. The main aim of this testing phase was to validate the performance of the various rig components compared to the numerical model calculations and identify potential material compatibility issues.

The 2kW preheater supplied a maximum temperature of 260°C at a flow rate of 15kg/h. A slow temperature response was observed when the mass flow rate was varied, resulting in a noticeable delay in achieving the temperature setpoint.

The heating section made of two sections of 940W heating tape, and a layer of Rockwool thermal insulation has successfully compensated for the heat loss by natural convection to the ambient air and satisfactorily heated the gas to a target temperature of 500°C. Quick response to temperature and mass flow variations was observed which mitigated the impact of the slow response of the preheater. Scenarios where supplying flow rates more than 15kg/hr at 500°C will require more sections of the heating tape.

The cooling bundle effectively dropped the gas temperature by ~315°C when the gas inlet temperature and flow rate were 500°C and 15kg/h, respectively. This drop is 1.8% more than the expected drop from the numerical model due to the conservative assumptions made in the numerical model regarding the fin efficiency, contact resistance, and ambient air heat transfer coefficient.

A steady-state operation is achieved by manually tuning the metering valve opening to satisfy the target temperature when the heating power is fixed. The results bring confidence in the selection of Cv values for back pressure devices. The recorded signal results and the tuning process show a high potential for successful process automation.

Despite the slow response of the preheater, the overall system response is satisfactory where the time needed to start up the system and achieve the 500°C conditions is less than 30 minutes. Minimal temperature overshooting of less than 1% of the design value is recorded by controlling the flow rate to maintain the maximum temperature at the design limit.

ACKNOWLEDGEMENT

This research was funded by the Department for Energy Security and Net Zero (DESNZ) under its grant funding agreement for Carbon Capture, Usage, and Storage Innovation 2.0, Project Reference CCUS 2108: "Innovative High-Temperature Sealing Solution for Supercritical CO_2 Power Cycles." The authors extend their gratitude to John Crane UK Limited and the University of Edinburgh for their invaluable support during the project. Special thanks go to Klaus Meck for his insightful contributions to this research effort, as well as to Kevin Howard and Stefania Romero for their dedication to the experimental test campaigns.

DOI: 10.17185/duepublico/83294

7 REFERENCES

[1] U. Sultan *et al.*, "Qualitative assessment and global mapping of supercritical CO2 power cycle technology," *Sustainable Energy Technologies and Assessments*, vol. 43, no. January, p. 100978, 2021, doi: 10.1016/j.seta.2020.100978.

[2] R. González-Almenara, P. R. de Arriba, F. Crespi, D. Sánchez, A. Muñoz, and T. Sánchez-Lencero, "Supercritical Carbon Dioxide Cycles for Concentrated Solar Power Plants: A Possible Alternative for Solar Desalination," *Processes*, vol. 10, no. 1, 2022, doi: 10.3390/pr10010072.

[3] A. S. Abdeldayem, S. I. Salah, M. T. White, and A. I. Sayma, "A Modified Loss Breakdown Approach for Axial Turbines Operating With Blended Supercritical Carbon Dioxide," *J Eng Gas Turbine Power*, vol. 145, no. 8, Jul. 2023, doi: 10.1115/1.4062478.

[4] P. Breeze, *Power Generation Technologies*. 2005. doi: 10.1016/B978-0-7506-6313-7.X5000-1.

[5] R. A. Dennis, G. Musgrove, G. Rochau, D. Fleming, M. Carlson, and J. Pasch, "Overview," in *Fundamentals and Applications of Supercritical Carbon Dioxide (sCO_2) Based Power Cycles*, K. Brun, P. Friedman, and R. Dennis, Eds., Woodhead Publishing, 2017, pp. xix–xxviii. doi: https://doi.org/10.1016/B978-0-08-100804-1.02001-6.

[6] A. Abdeldayem *et al.*, "Integrated Aerodynamic and Mechanical Design of a Large-Scale Axial Turbine Operating With A Supercritical Carbon Dioxide Mixture," *J Eng Gas Turbine Power*, vol. 146, no. 2, Nov. 2023, doi: 10.1115/1.4063530.

[7] E. Anselmi, V. Pachidis, M. Johnston, I. Bunce, and P. Zachos, "An Overview of the Rolls-Royce sCO 2-Test Rig Project at Cranfield University," in *Proceedings of the 6th International sCO2 Power Cycles Symposium, 27 - 29th March*, 2018.

[8] J. A. Bennett, W. Paudel, A. F. Clarens, B. Weaver, and C. Watson, "Computational analysis of seals for sCO2 turbomachinery and experimental planning," in *The 6th International Supercritical CO2 Power Cycle Symposium*, 2018, p. 22503.

[9] J. Nielson, T. Kerr, B. Hellmig, A. Fesl, A. Laxander, and P. Philippi, "Component Testing of a High Temperature Dry Gas Seal," *The 7th International Supercritical CO2 Power Cycles Symposium*, pp. 1–14, 2022.

[10] D. Steinmann, R. Kassimi, J. Kleiner, P. Susini, A. Milani, and M. Dozzini, "Dry gas seals design for centrifugal compressors in supercritical CO2 application," in *7th International sCO2 Power Cycles SymposiumSan Antonio, Texas*, 2022.

[11] A. Rimpel *et al.*, "Test rig design for large supercritical CO2 turbine seals," in *The Sixth International Supercritical CO2 Power Cycle Symposium*, 2018, pp. 1–14.

[12] A. Laxander, "Development and testing of dry gas seals for turbomachinery in multiphase CO2 applications," in *The 3rd European supercritical CO2 conference*, Paris: Deutsche Nationalbibliothek, Sep. 2019.

[13] R. Yan, H. Chen, W. Zhang, X. Hong, X. Bao, and X. Ding, "Calculation and verification of flow field in supercritical carbon dioxide dry gas seal based on turbulent adiabatic flow model," *Tribol Int*, vol. 165, p. 107275, 2022.

[14] S. Cich, J. Moore, and M. Day-Towler, "CSP11-Testing and Troubleshooting of Pump Dry Gas Seals Operating with sCO2," in *Proceedings of the 48th Turbomachinery Symposium*, Turbomachinery Laboratory, Texas A&M Engineering Experiment Station, 2019.

[15] GOV.UK, "Carbon Capture, Usage and Storage (CCUS) Innovation 2.0: Innovative high temperature sealing solution for supercritical CO_2 power cycle." Accessed: Jul. 06, 2024. [Online]. Available: https://www.gov.uk/government/publications/carbon-capture-usage-and-storage-ccus-innovation-20-competition-call-1-successful-projects/carbon-capture-usage-and-storage-ccus-innovation-20-competition-call-2-successful-projects

[16] Parker AutoClave, "Technical Information: Pressure/Temperature Rating Guide," 2016. Accessed: Jul. 06, 2024. [Online]. Available: https://www.autoclave.com/products/technical_information/pressure_temperature_rating/index.html

[17] E. Sterner and U. Wickström, *TASEF-temperature analysis of structures exposed to fire. User's manual.* Fire Technology, SP REPORT, 1990:05, 1990.

[18] Y. A. Cengel and A. J. Ghajar, *Heat and Mass Transfer - Fundamentals and Applications - Fifth Edition*. 2015.

[19] MathWorks, "Simulink." Accessed: Nov. 15, 2024. [Online]. Available: https://uk.mathworks.com/products/simulink.html

[20] Parker Autoclave, "Item # 30VRMM4812, VRMM Series MicroMetering Needle Valves." Accessed: Nov. 15, 2024. [Online]. Available: https://parker.autoclave.com/item/micrometering-valves/vrmm-series-micrometering-needle-valves/30vrmm4812-1

[21] Swagelok, "Metering Valves." [Online]. Available: https://www.swagelok.com/downloads/webcatalogs/en/ms-01-142.pdf

[22] H. Yuan and M. Anderson, "Experimental and numerical study of supercritical carbon dioxide flow through valves," *Journal of Nuclear Engineering and Radiation Science*, vol. 2, no. 3, pp. 1–8, 2016, doi: 10.1115/1.4032640.

DOI: 10.17185/duepublico/83294

Design challenges and preliminary test results of a high temperature supercritical carbon dioxide dry gas seal test rig

Abdeldayem, Abdelrahman

2025-04-09

Abdeldayem A, Kissoon S, Palma EA. (2025) Design challenges and preliminary test results of a high temperature supercritical carbon dioxide dry gas seal test rig. Proceedings of the European Sco2 Conference. 6th European Conference on Supercritical CO2 (sCO2) for Energy Systems, 9-11 April 2025, Delft, Netherlands, pp. 130-140

https://doi.org/10.17185/duepublico/83294